UNITED NATIONS EDUCATIONAL, SCIENTIFIC AND CULTURAL ORGANIZATION
INTERNATIONAL ATOMIC ENERGY AGENCY
INTERNATIONAL CENTRE FOR THEORETICAL PHYSICS
I.C.T.P., P.O. BOX 586, 34100 TRIESTE, ITALY, CABLE: CENTRATOM TRIESTE

SMR.998a - 9

Research Workshop on Condensed Matter Physics
30 June - 22 August 1997
MINIWORKSHOP ON
QUANTUM MONTE CARLO SIMULATIONS OF LIQUIDS AND SOLIDS
30 JUNE - 11 JULY 1997
and
CONFERENCE ON
QUANTUM SOLIDS AND POLARIZED SYSTEMS
3 - 5 JULY 1997

"Path integral simulations of quantum clusters"

C. CHAKRAVARTY
Department of Chemistry
Indian Institute of Technology
Hauz Khas
New Delhi 110016
INDIA

These are preliminary lecture notes, intended only for distribution to participants.

PATH INTEGRAL SIMULATIONS OF QUANTUM CLUSTERS

PATH INTEGRAL MONTE CARLO METHODS

- Finite temperature properties of quantum many-body systems
- Canonical ensemble
- Equilibrium static properties
- Exact for distinguishable quantum particles and bosons
- Approximations necessary for fermions
- Extracting dynamical information is problematic

CLUSTERS

- 10 to 10^4 atoms
- Transition from molecular to bulk limit
- Insights into phase transitions, nucleation and solvation
- Quantum clusters:
  Quasiclassical: Ne_n, $(N_2)_n$, Ar_n
  Large quantum effects: He_n, $(H_2)_n$, $(D_2)_n$
  Hydrogen-bonded clusters: $(HF)_n$, $(NH_3)_n$, $(H_2O)_n$

- Fourier path integral Monte Carlo simulations
- Quantum effects on cluster melting
- Binary isotopic mixtures
- Instantaneous normal mode spectra
- Helium in zeolites

Path Integral Representation of the Density Matrix

Canonical Partition Function

$$Z = \mathrm{Tr}\{ e^{-\beta \hat{H}} \} , \quad \beta = 1/k_B T$$

$$= \int d\vec{x} \, \langle \vec{x} | e^{-\beta \hat{H}} | \vec{x} \rangle , \quad \hat{H} = \hat{K} + \hat{V}$$

Trotter discretisation

$$e^{-\beta \hat{H}} = \lim_{M \to \infty} \left[e^{-\varepsilon \hat{K}} e^{-\varepsilon \hat{V}} \right]^M$$

Inserting $M-1$ complete sets of states

$$Z = \int \prod_{i=0}^{M-1} d\vec{x}_i \, \langle \vec{x}_i | e^{-\frac{\beta}{M}\hat{K}} e^{-\frac{\beta}{M}\hat{V}} | \vec{x}_{i+1} \rangle$$

Primitive Approximation

$$Z = \int \prod_{i=0}^{M-1} \left(d\vec{x}_i \; e^{-\frac{mM}{2\beta\hbar^2}(\vec{x}_i - \vec{x}_{i+1})^2 - \frac{\beta}{M} V(\vec{x}_i)} \right)$$

$$= \int d\vec{x}_0 \ldots \quad d\vec{x}_{M-1} \, e^{-\frac{mM}{2\beta\hbar^2} \sum_{i=0}^{M-1} (\vec{x}_i - \vec{x}_{i+1})^2 - \frac{\beta}{M} \sum_{i=0}^{M-1} V(\vec{x}_i)}$$

Path Integral Representation of the density matrix

$$Z = \int \mathcal{D}(x(u)) \; e^{-\frac{1}{\hbar} \int_0^{\beta\hbar} [K(x(u)) + V(x(u))] \, du}$$

$$= \int \mathcal{D}(x(u)) \; e^{-S(x(u))}$$

FOURIER PATH INTEGRAL REPRESENTATION

The Fourier path integral approach introduces a set of auxilliary variables which represent different length scale fluctuations of the quantum paths .

Classical free particle path: $\mathbf{x}_c(u) = \mathbf{x}_i + (\mathbf{x}_f - \mathbf{x}_i)(u/\beta\hbar)$.

Fluctuations about reference path:

$$\mathbf{y}(u) = \sum_{k=1}^{k_{max}} \mathbf{a}_k \sin(k\pi u/\beta\hbar)$$

auxilliary variables

$-S(x(u)) = \int K(x(u)) + V(x(u))$

Partition function

$$Z = J \int d\mathbf{x} d\mathbf{a} \exp(-\sum_k \frac{\mathbf{a}_k^2}{2\sigma_k^2} - \beta V_{eff})$$

- Quantum-classical isomorphism is retained.
- Metropolis variables: $3N$ spatial coordinates, $\mathbf{x}$
  $3N\,k_{max}$ Fourier coefficients, $\mathbf{a}$
- Quantum fluctuations
  Length scale associated with Fourier coefficent of order k, $\sigma_k = \sqrt{2\beta\hbar^2/m\,k^2\pi^2}$
- Potential energy evaluated along path:

$$V_{eff} = (1/\beta\hbar)\int_0^{\beta\hbar} V(\mathbf{x}(u))du$$

- The kinetic energy term is decoupled into contributions from $3N\,k_{max}$ independent degrees of freedom.

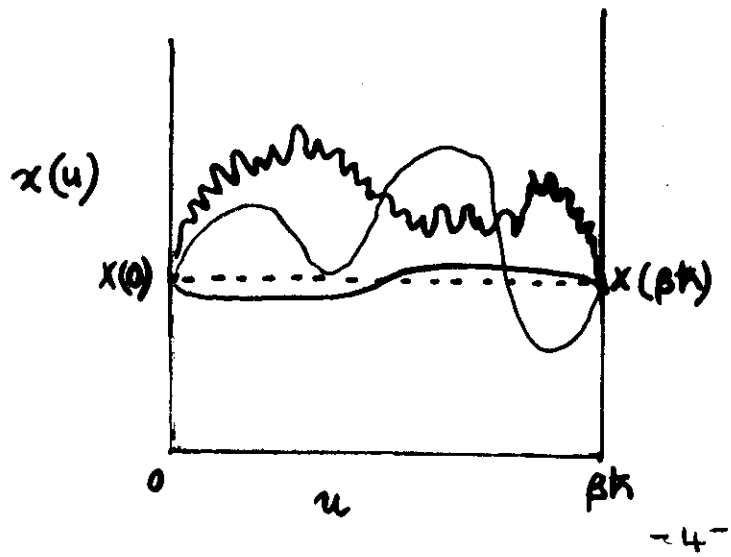

Doll, Coalson & Freeman (1985)

PARTIAL AVERAGING

High frequency Fourier modes, with $k \geq k_{max}$, represent very small length scale fluctuations and are treated as Gaussian variables.

Any linear combination $p = \Sigma_k \lambda_k b_k$ where b_k is a Fourier coefficient with $k > k_{max}$ corresponds to a single Gaussian variable p with variance $\Sigma_k \lambda_k^2 \sigma_k^2$.

Therefore

$$\mathcal{Z} = J \int d\mathbf{x} d\mathbf{a} \exp(-\sum_{k=1} \frac{\mathbf{a}_k^2}{2\sigma_k^2}) \langle \exp(-\beta V_{eff}) \rangle_G$$

where

$$\langle \exp(-\beta V_{eff}) \rangle_G = \int dp \exp(-\frac{p^2}{2\sigma^2(u)}) \exp(-\beta V_{eff}(\mathbf{x}(u) + p).$$

$$\mathbf{x}(u) = \mathbf{x}_i + \sum_{k=1}^{k_{max}} a_k \sin(k\pi u/\beta\hbar)$$

$$\sigma^2(u) = \frac{\beta\hbar^2}{m}[u(1-u) - \frac{2}{\pi^2} \sum_{k=1}^{k_{max}} \frac{\sin^2(k\pi u/\beta\hbar)}{k^2}]$$

Using the Gibbs-Boguliobov inequality, one can write

$$\langle \exp(-\beta V_{eff}) \rangle_G \geq \exp(-\beta \langle V_{eff} \rangle_G)$$

For any multi-dimensional system one can show that the RHS of the above inequality can be evaluated to second-order in p as

$$V_{eff} = (1/\beta\hbar) \int_0^{\beta\hbar} du (V(\mathbf{x}(u)) + \underbrace{\sum_{i=1}^{3N} 0.5\sigma^2(u) V_{ii}(\mathbf{x}(u))}$$

Quantum correction $\propto \frac{\beta\hbar^2}{m}$

Diagonal matrix elements of the Hessian.

Quantities Derived from Simulations

- Structural Quantities

  $\hat{O}$: diagonal in coordinates

  Lindeman index
  Density profile
  Potential energy

$$\langle O \rangle = \frac{Tr\{\hat{O}\, e^{-\beta \hat{H}}\}}{Tr\{e^{-\beta \hat{H}}\}} = \frac{\int d\vec{x}\, d\vec{\alpha}\; O(x)\, e^{-\sum_k \frac{a_k^2}{2\sigma_k^2} - \beta V_{eff}}}{\int d\vec{x}\, d\vec{\alpha}\; e^{-\sum_k \frac{a_k^2}{2\sigma_k^2} - \beta V_{eff}}}$$

- Total Energy

$$\langle E \rangle = -\frac{\partial (\ln Z)}{\partial \beta} = \frac{3N(k_{max}+1)}{2\beta} - \left\langle \sum_k \frac{a_k^2}{2\sigma_k^2 \beta} \right\rangle_{MC} + \langle V_{eff.} \rangle_{MC}$$

- Kinetic Energy

$$\langle K \rangle = \frac{m}{\beta} \frac{\partial (\ell n Z)}{\partial \beta} = \frac{3N(k_{max}+1)}{2\beta} - \left\langle \sum_k \frac{a_k^2}{2\rho\sigma_k^2} \right\rangle_{MC}$$

- Specific Heat

$$C_v / k_B = -\beta^2 \frac{\partial^2 (\ell n Z)}{\partial \beta^2}$$

CLUSTER SOLID-LIQUID TRANSITION

- Lindemann index is a better order parameter than long-range translational order
- Magic numbers:
  Lennard-Jones: 7,13,19,55,147,309,... (or any other pair potential)
  Geometric or packing considerations
  Alkali metals: 8,18,20,40,58,92, ...
  Electronic structure considerations
- Interesting analogue of bulk melting shown by magic number clusters
  $T < T_f$: solid-like phase
  $T > T_m$: liquid-like phase
  $T_f < T < T_m$: dynamical coexistence regime
- Solid-like phase: rigid, small Lindemann index
  Liquid-like phase: non-rigid, large Lindemann index
- $T_f, T_m <$ Bulk melting temperature

Experimental evidence

- Electron Microscopy of metal clusters

  Can observe shape fluctuations in supported metal clusters on timescale of < 0.1s

  Iijima *et al*, Phys.Rev.Lett., **56**, 616 (1986).

- Mass abundance spectra: Xe_N, Ar_N, Na_N, Au_N ...

  Identify magic numbers

  Evidence for size dependent melting of Na clusters

  T.P.Martin *et al*, J.Chem.Phys., **100** (1994)

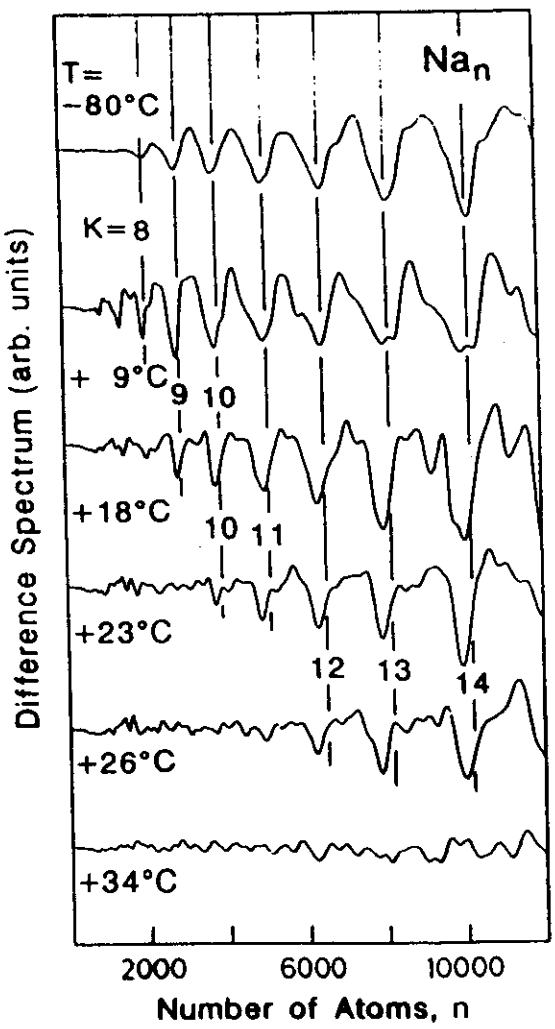

Alkali clusters:

Small sizes:
Electronic structure determines magic number

Large sizes:
Geometric Packing

- Clusters doped with a chromophore

  Argon$_N$-benzene clusters, Argon$_N$-SF_6

  Monitor chromophore transition

  Dependence of spectroscopic line shape on N

  Hahn & Whetten, Phys.Rev.Lett.,**61**,1190(1988).

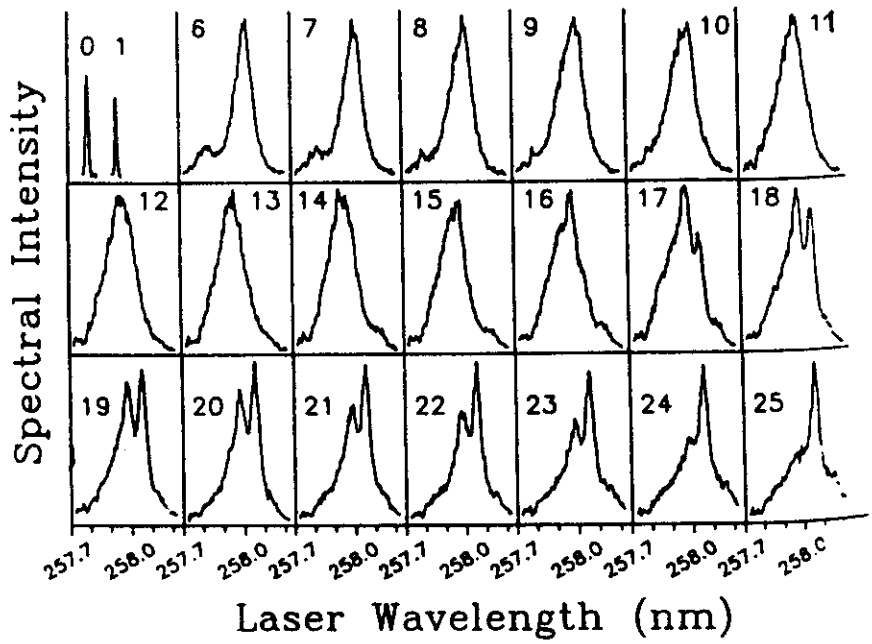

Classical $(LJ)_{13}$ Cluster

Potential parameters are for Neon

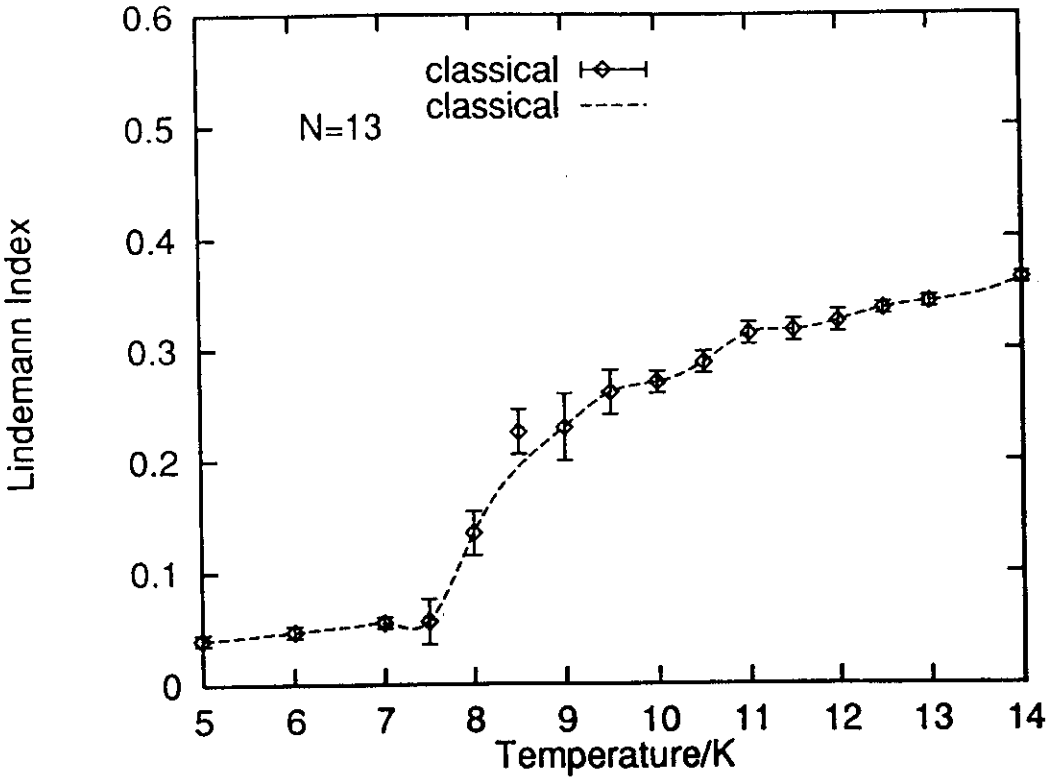

Bulk melting temp. = 24 K.

Magic numbers
13, 19, 55, 147
.....

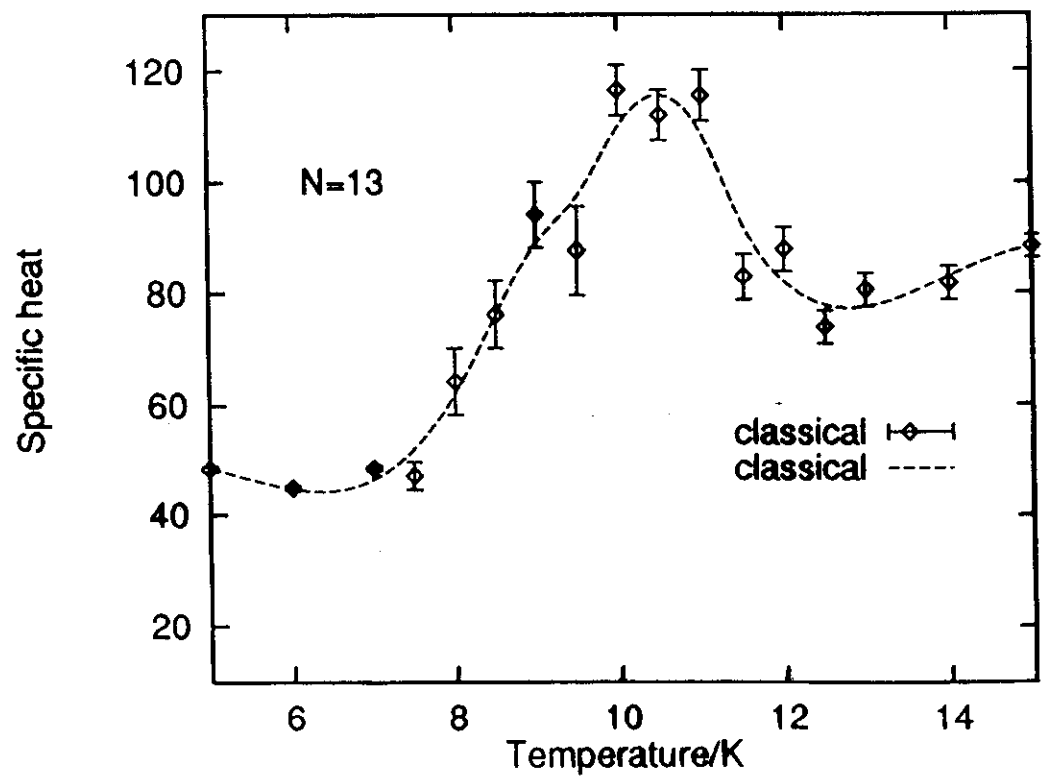

Potential Energy Surface.

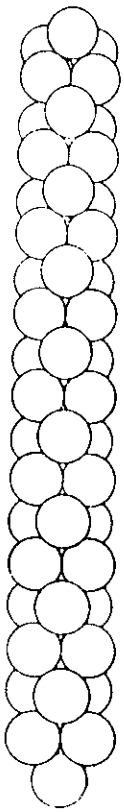

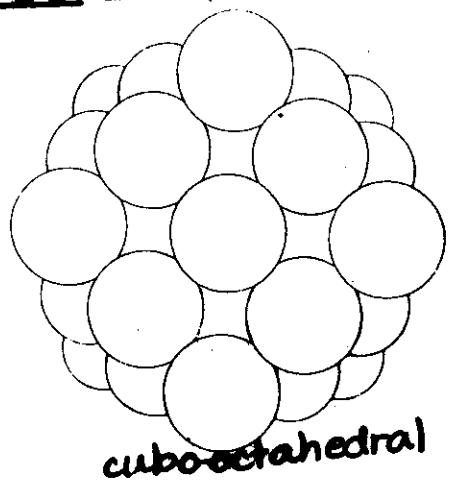

cuboctahedral

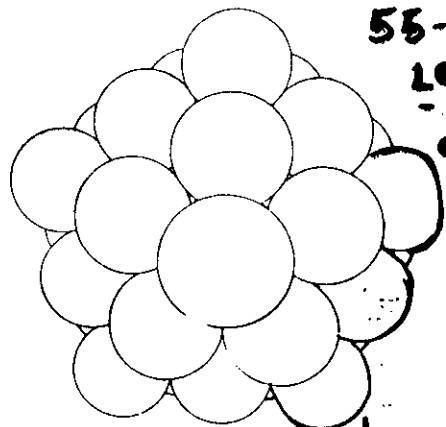

icosahedral.

55-atom Lennard-Jones cluster

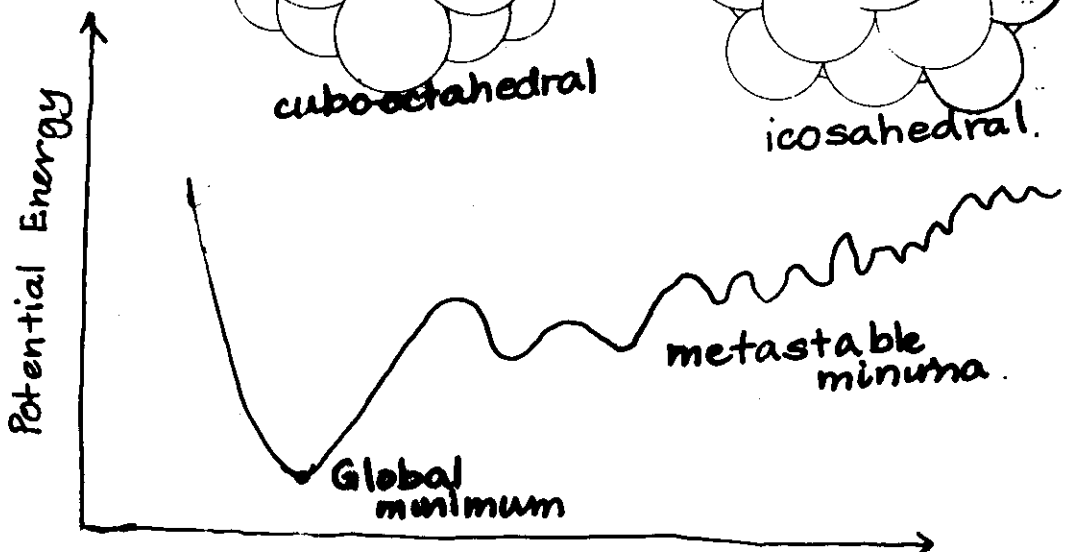

Magic number clusters: Large separation between global and metastable minima.

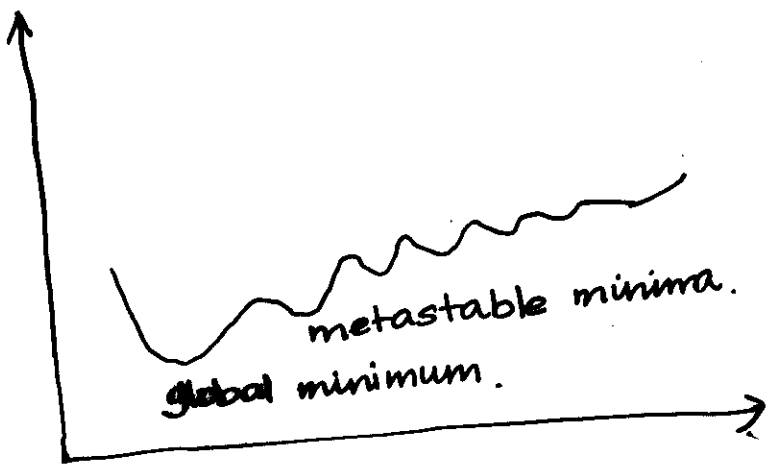

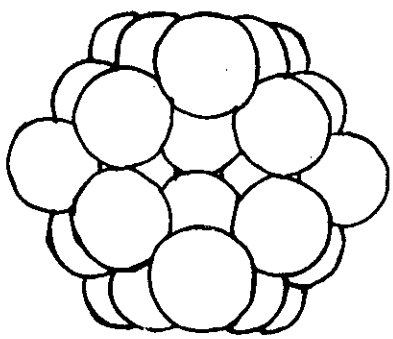

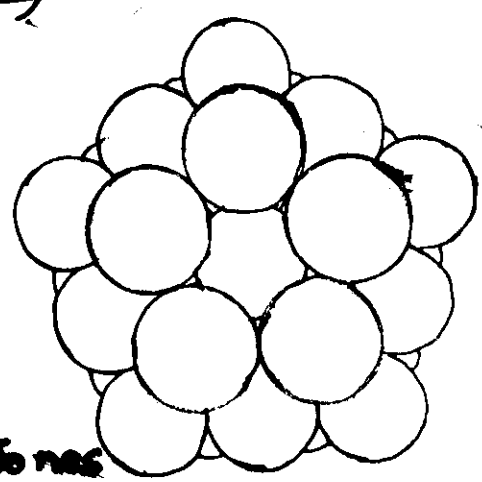

54-atom Lennard-Jones cluster

QUANTUM EFFECTS ON CLUSTER MELTING

Classical Principle of Corresponding States

For identical functional forms of the pair potential, the equilibrium properties of classical systems will be identical when measured in reduced units

Quantum Lennard-Jones Systems

- Parameters: m, ϵ, σ
- Thermal de Broglie wavelength
  $\lambda_T = \hbar/\sigma\sqrt{m\epsilon T^*}$
- de Boer parameter
  $\Lambda = \hbar/\sigma\sqrt{m\epsilon}$

	Λ	ϵ/ K	σ /Å	m/amu
Neon	0.095	35.6	2.75	20
o-D_2	0.201	34.2	2.96	4
p-H_2	0.284	34.2	2.96	2
^{4}He	0.427	10.2	2.55	4

- Quantum effects on the cluster solid-liquid transition?

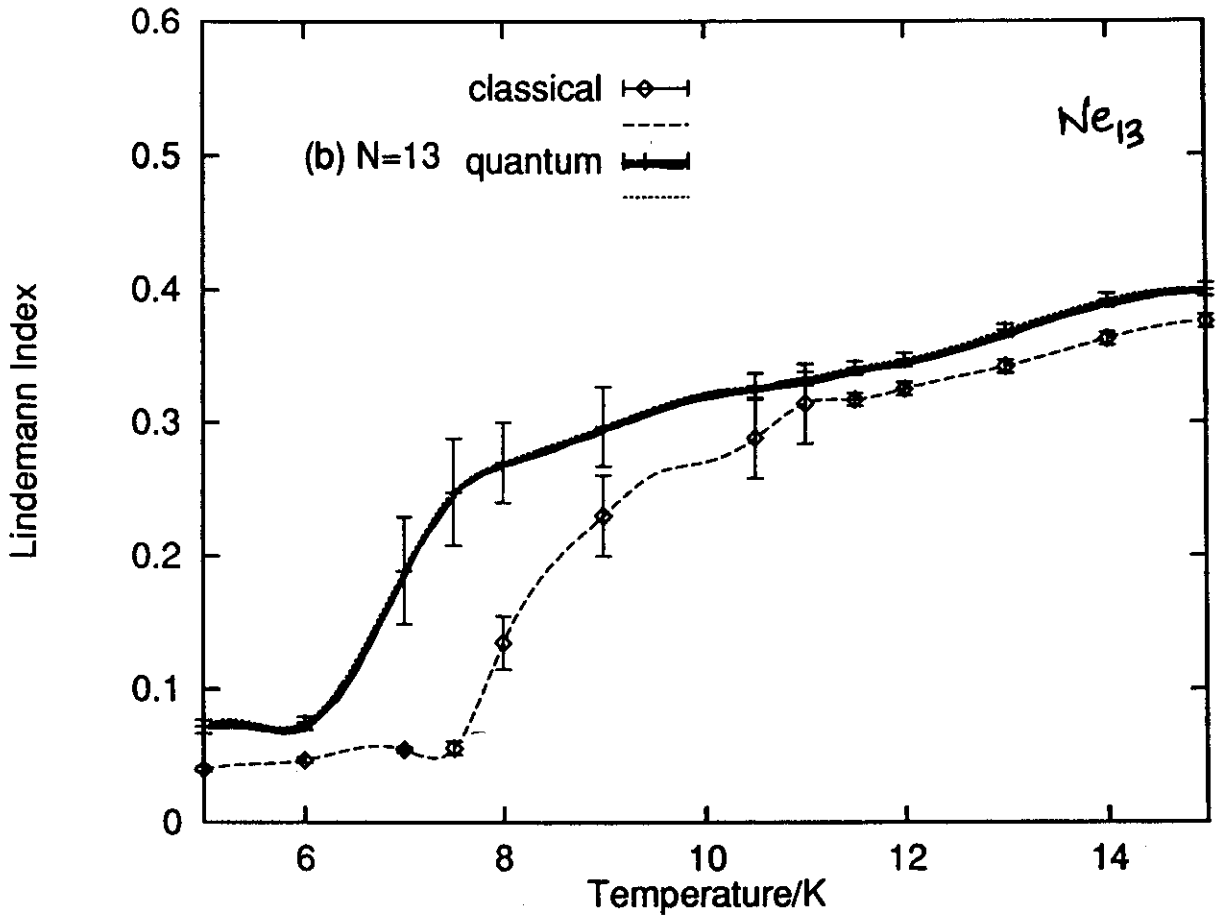

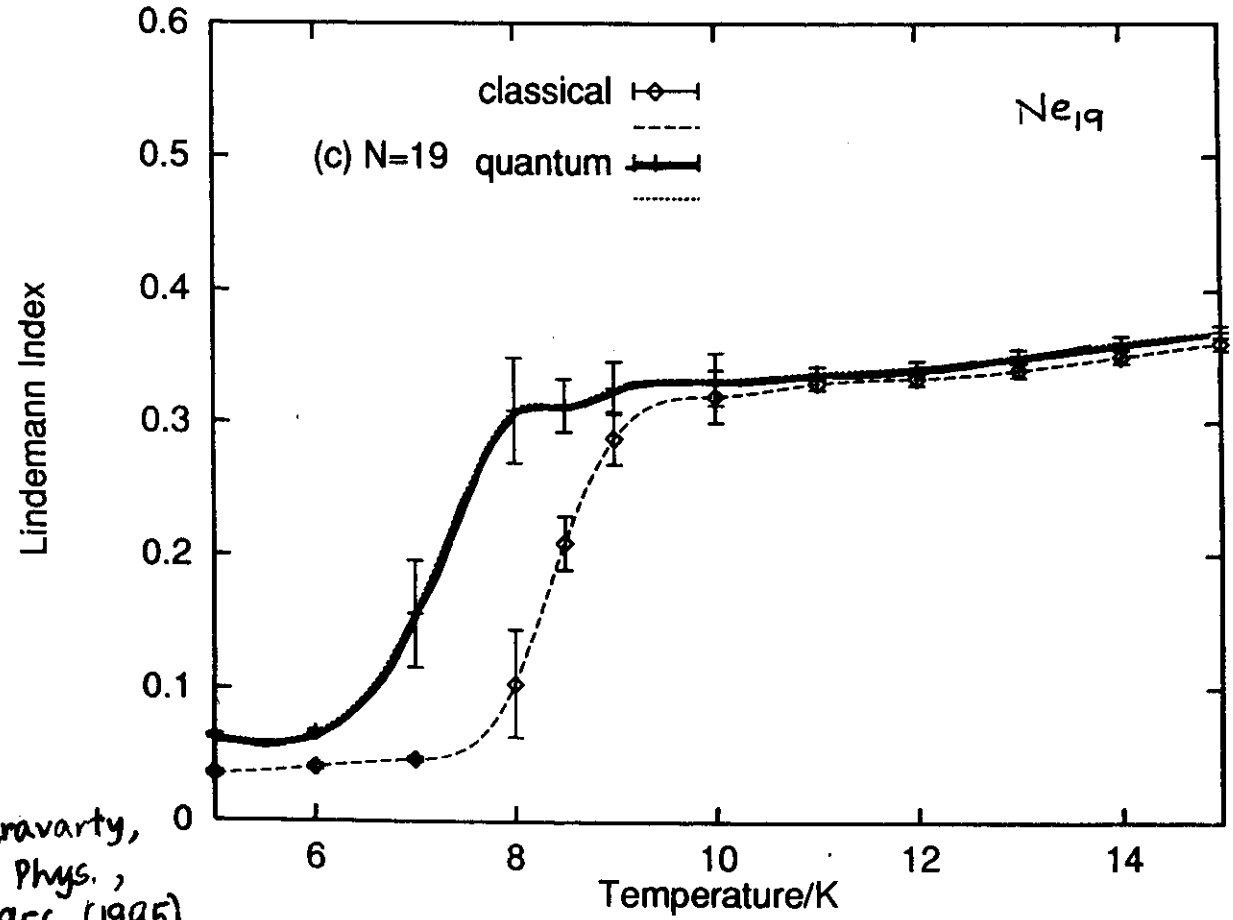

C. Chakravarty, J. Chem. Phys., 102, 956 (1995).

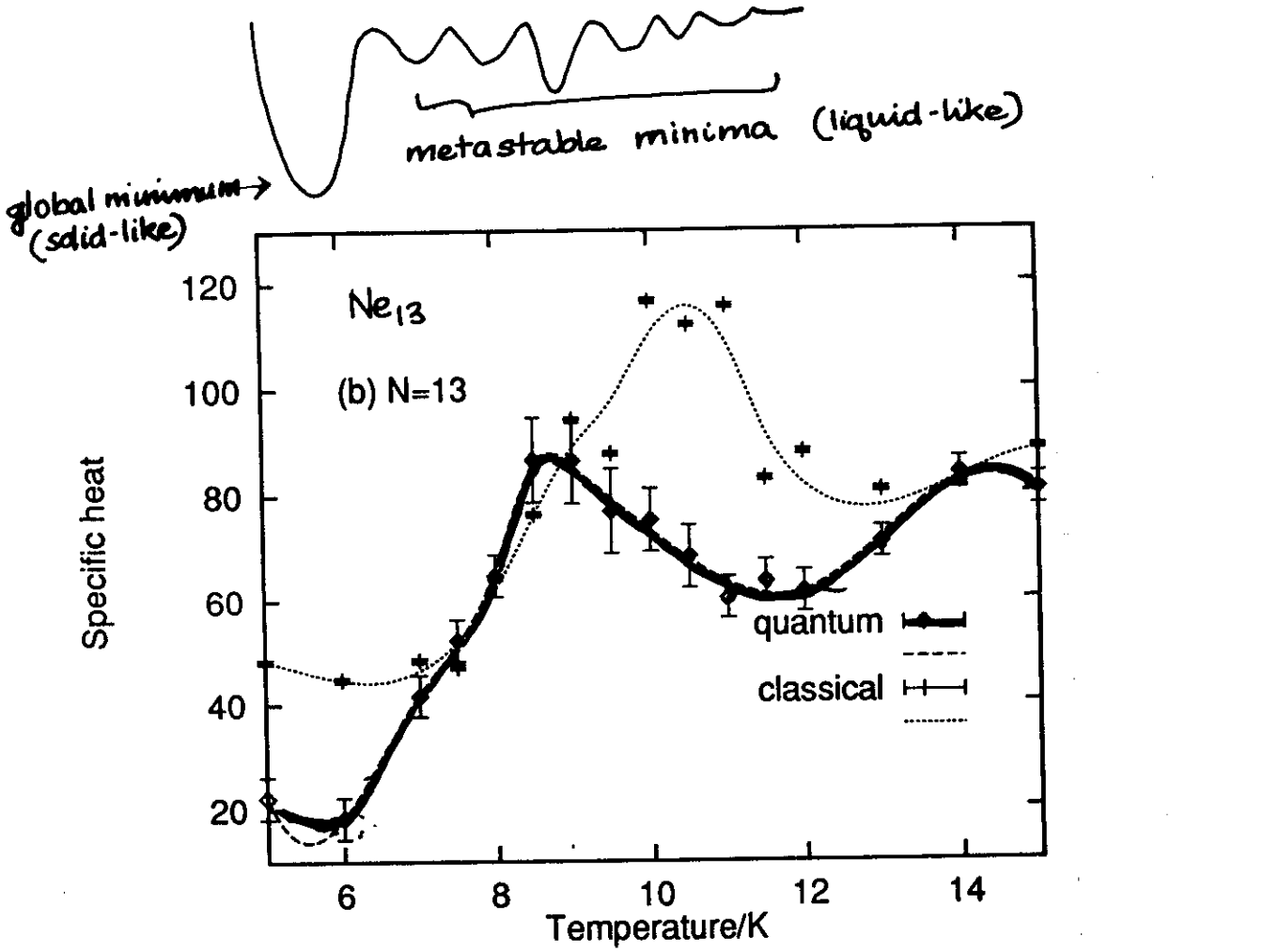

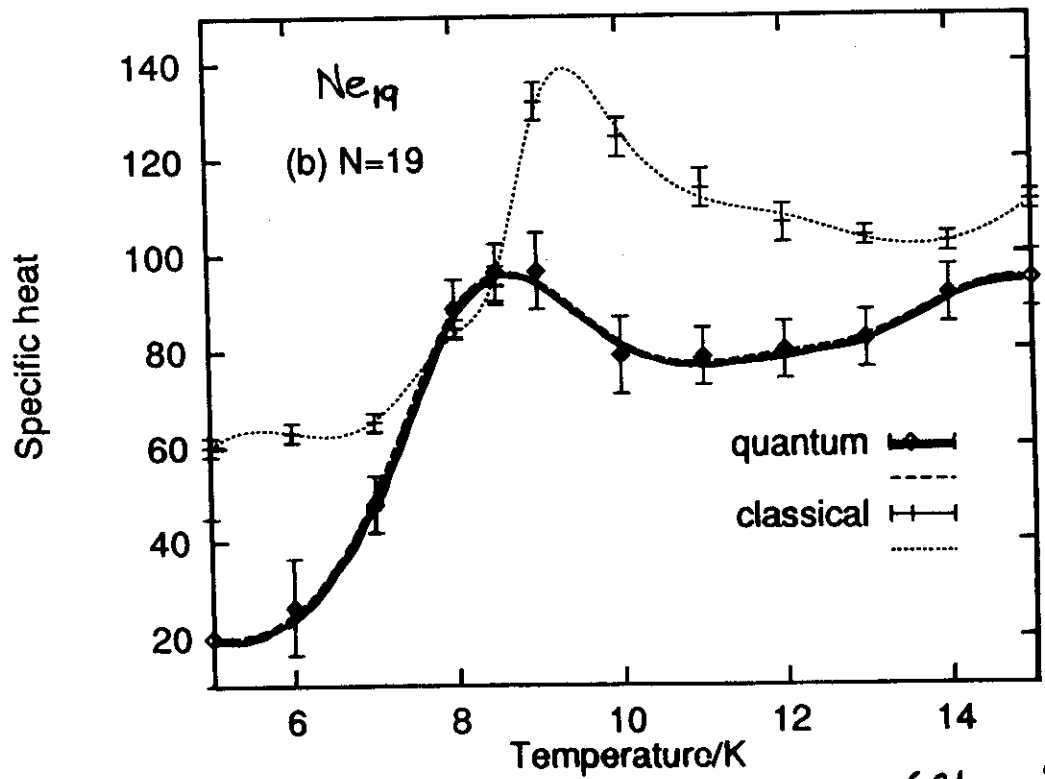

C. Chakravarty, J. Chem. Phys. Vol. 102, 956 (1995)

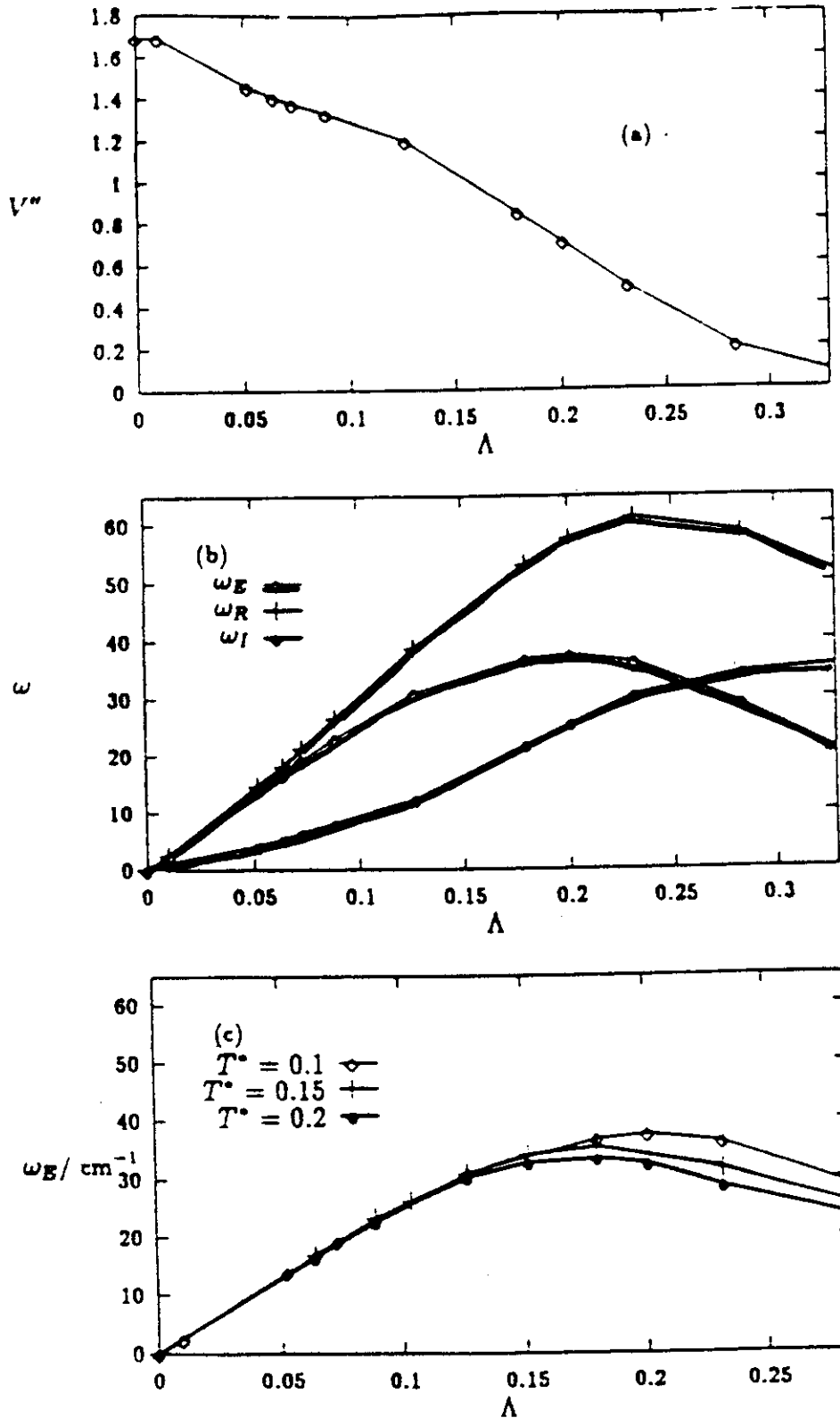

Average force constant.

Chakravarty & Ramaswamy, J. Chem. Phys., 1997.

FIG. 3. (a) The average force constant, $(V'')/10^{-2}$, in atomic units, as a function of Λ. (b) The Einstein frequency, ω_E (in cm^{-1}), and its real, ω_R, and imaginary components, $|\omega_I|$, are plotted as a function of Λ. All frequencies are in units of cm^{-1}. Errors in ω_E are of the order of ± 2 cm^{-1}. (c) The Einstein frequency, ω_E (in cm^{-1}), as a function of Λ for $T^* = 0.1$, 0.15, and 0.2. All frequencies are in units of cm^{-1}. Errors in ω_E are of the order of ± 2 cm^{-1}.

$\frac{kT}{\varepsilon} = 0.15$

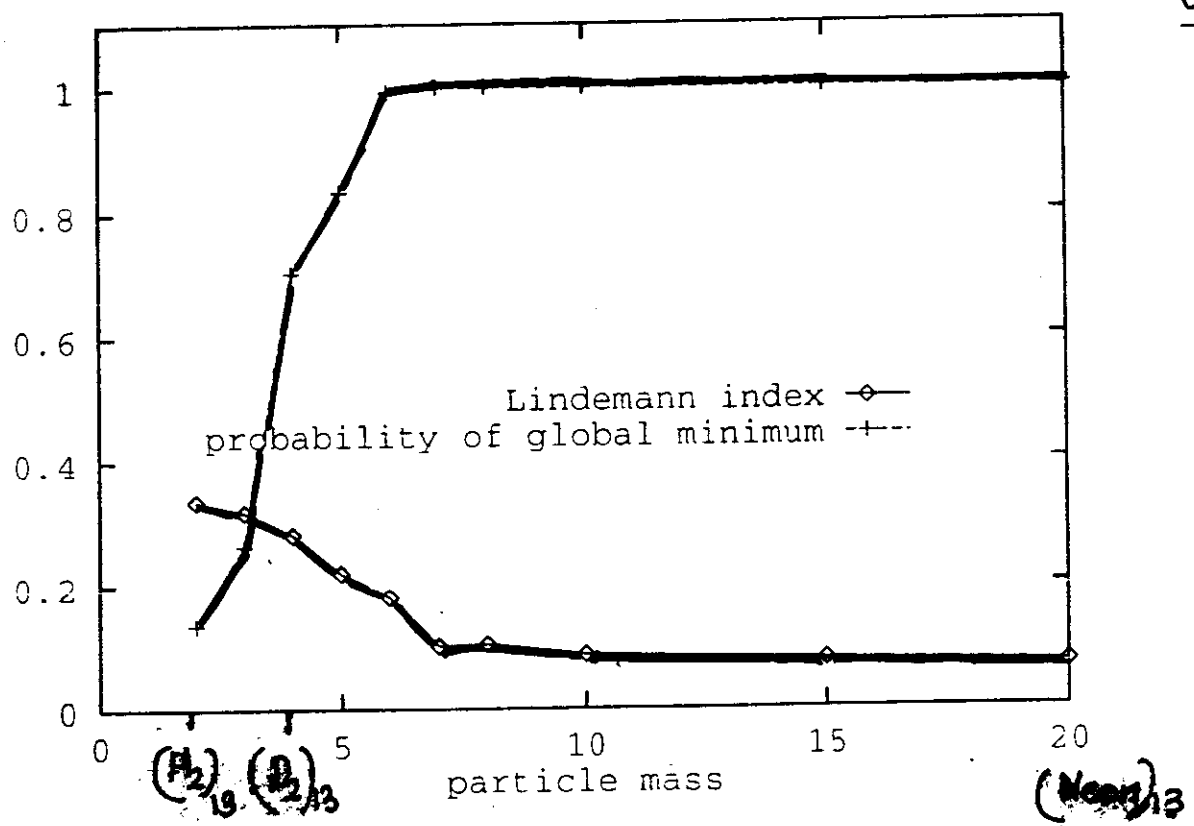

Cluster Solid-liquid Transition induced by Quantum fluctuations

Kinetic energy contribution due to quantum effects plays the same role as the thermal kinetic energy.

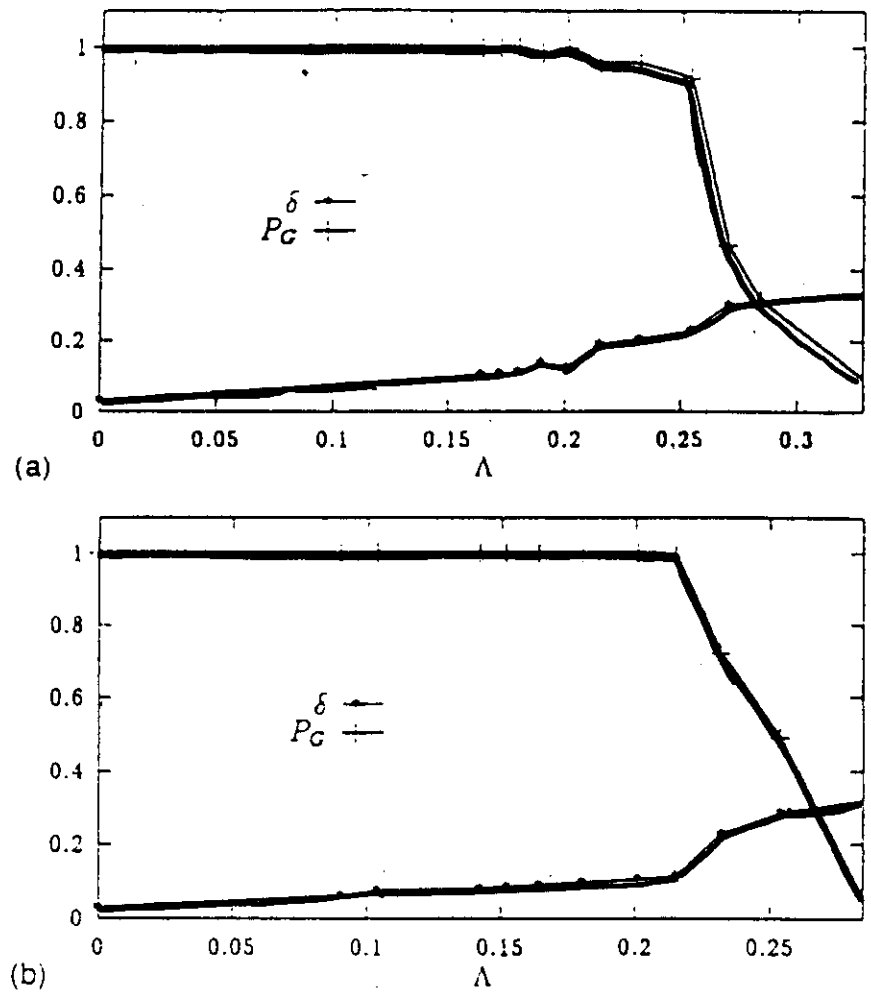

FIG. 4. The probability of occupation of the global minimum, P_G, and the Lindemann index, δ, as a function of Λ for (a) $(LJ)_{13}$ and (b) $(LJ)_{19}$.

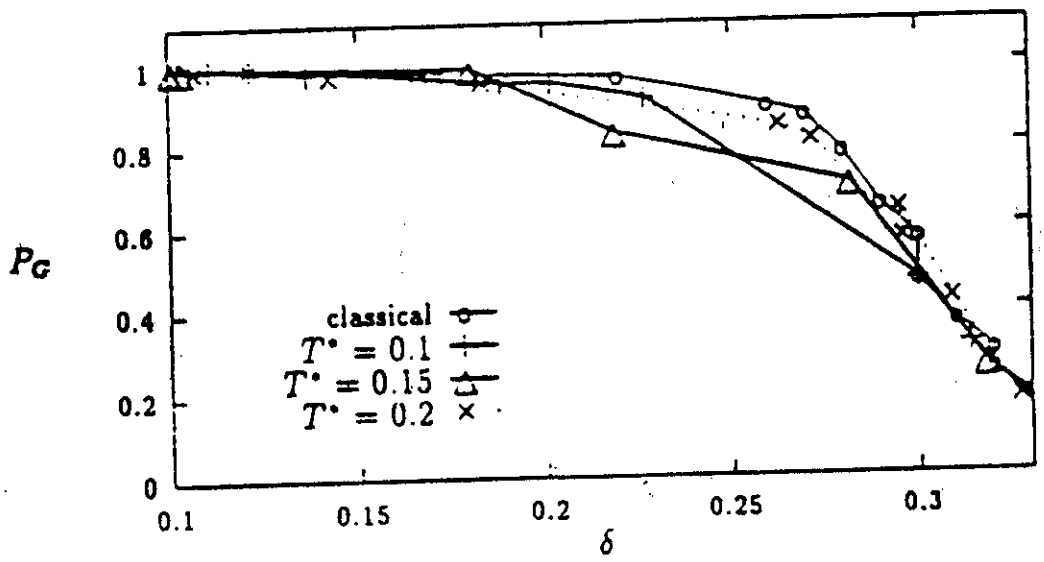

FIG. 5. The probability of occupation of the global minimum, P_G, as a function of the Lindemann index, δ, for $(LJ)_{13}$ for the classical thermal CSLT and for the QCSLT at different reduced temperatures.

Reduced Temperature $= T^* = \frac{k_B T}{\varepsilon}$: Thermal fluctuations

de Boer parameter $= \Lambda = \hbar / \sigma\sqrt{m\varepsilon}$: Quantum fluctuations

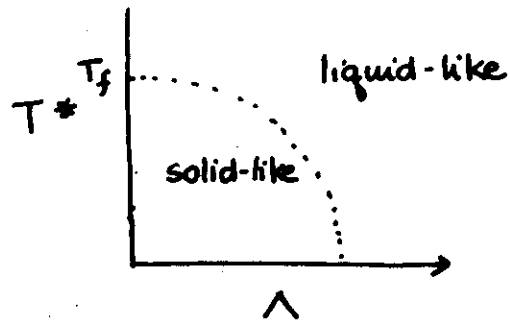

Figure 1

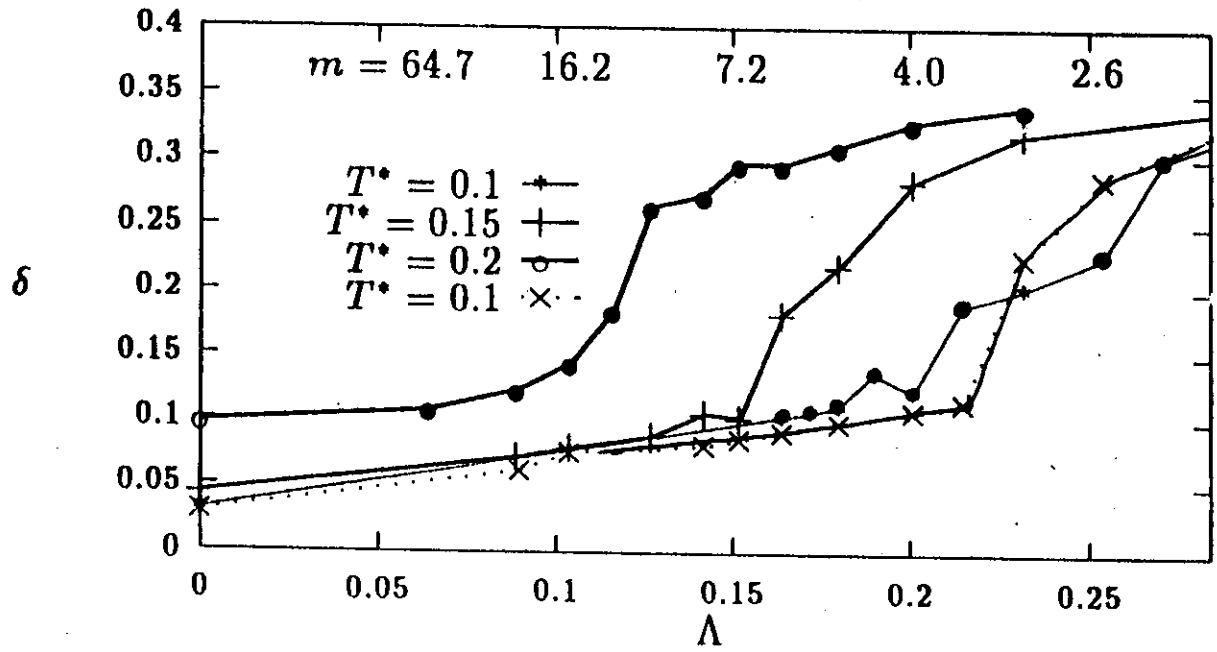

^4He $\Lambda = 0.427$

H_2 $\Lambda = 0.284$

D_2 $\Lambda = 0.201$

Ne $\Lambda = 0.095$

CH_4 $\Lambda = 0.037$

Ar $\Lambda = 0.028$

C. Chakravarty,
J. Chem. Phys. (1995)

QUANTUM CLUSTERS OF BINARY ISOTOPIC MIXTURES

Binary Phase Separation in Classical Mixtures

Two species A & B:

Energy parameters: $\epsilon_{AA}, \epsilon_{AB}, \epsilon_{BB}$

Size parameters: $\sigma_{AA}, \sigma_{AB}, \sigma_{BB}$

For a binary system, with

$\sigma_{AA} \approx \sigma_{AB} \approx \sigma_{BB}$

$\epsilon_{AA} < \epsilon_{AB} < \epsilon_{BB}$

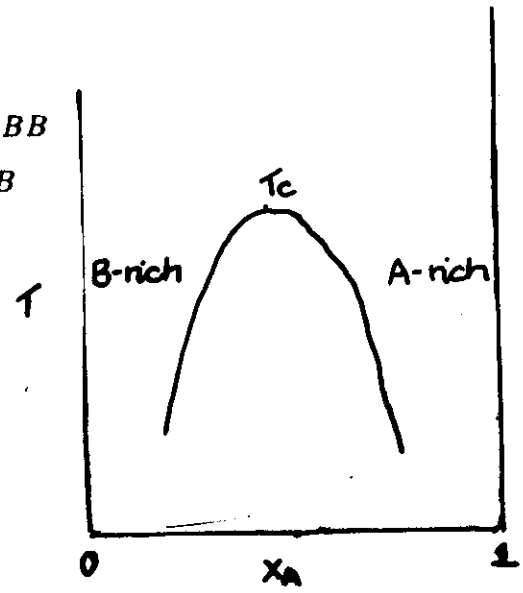

Cluster Analogue

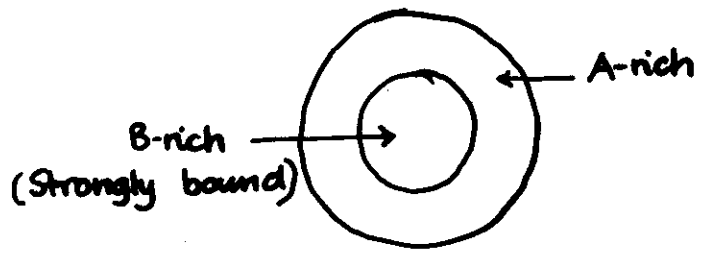

PRL, 1993 ; JCP (1994
Clarke, Capral & Patey,

QUANTUM ANALOGUE OF CLASSICAL PHASE SEPARATION

Isotopic mixture, A & B, with masses $m_A < m_B$

Classical limit: homogeneous

Quantum delocalization effects

Dimer at 0K:

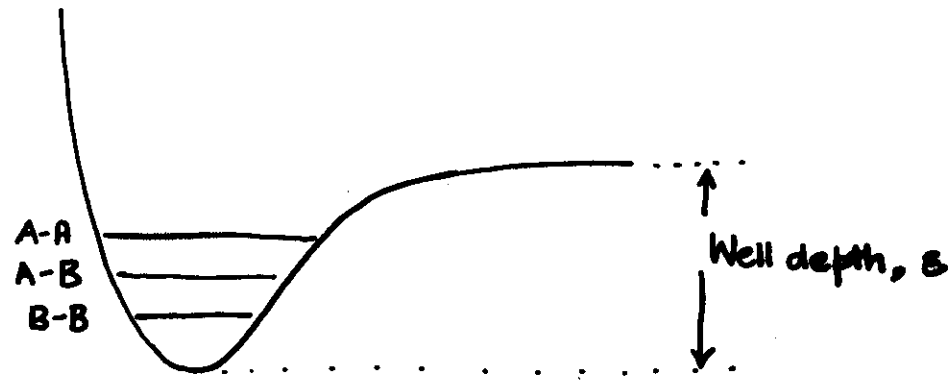

Zero-point energies:

$E^0_{AA} \propto \sqrt{2/m_A}$

$E^0_{AB} \propto \sqrt{2(m_A + m_B)/m_A m_B}$

$E^0_{BB} \propto \sqrt{2/m_B}$

Therefore, if $m_A < m_B$,

$$\epsilon_{AA} < \epsilon_{AB} < \epsilon_{BB}$$

$$\sigma_{AA} \approx \sigma_{AB} \approx \sigma_{BB}$$

Expect a spherical shell structure with the heavier isotope concentrated in the cluster core.

ISOTOPIC MIXTURES

- ^{3}He/^{4}He mixtures
  - Does show binary segregation in bulk isotopic mixtures
  - Complicated by the strong bosonic/fermionic character

- *ortho*-D_2/ *para*-H_2 mixture
  - Nuclear spin statistics implies that at low temperatures only the $J = 0$ state is occupied
  - pseudo-atomic Lennard-Jones systems with $\epsilon = 34.2$K and $\sigma = 2.96$Å
  - Bosonic system but identical particle exchange is negligible above 2 K
  - More accurate pair potentials: Silvera-Goldman etc.

- ^{20}Ne/ ^{22}Ne mixture
  - Quasiclassical system
  - Lennard-Jones parameters: $\epsilon = 35.6$ K and $\sigma = 2.75$Å

PIMC FOR A BINARY QUANTUM MIXTURE

Path Swapping

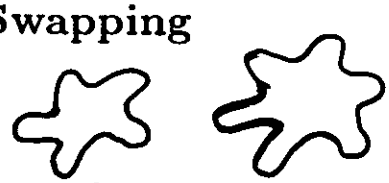

Parameteric Multistage Sampling

Use configurations sampled from a more ergodic distribution to equilibriate a less ergodic distribution.

- Reference System (RS)/ System of Interest (SI) e.g $para$-H_2/$ortho$-D_2.
- SI: characteristic parameters: β, m_A, m_B
- RS: characteristic parameters: β, m'_A, m'_B
- Equilibriate RS using path swapping moves and store a set of configurations, $\mathbf{X}_R = \{\mathbf{x}, \mathbf{a}\}$
- Equilibriation of SI:
  Usual Metropolis FPIMC
  + Occassional Jump Moves, $\mathbf{X} \rightarrow \mathbf{X}_R$
- Transition matrix for jump moves

$$T(\mathbf{x} \rightarrow \mathbf{x}_R) = e^{-S_R(\mathbf{x}_R)}$$

- Reference distribution can be stored or generated in tandem

Single Impurity in a cluster of $o\text{-}D_2$: $A\,(o\text{-}D_2)_N$

"One-particle" effective potential : $V_{eff}(R_i) = \left\langle \sum_{j \neq i} V_{ij} \right\rangle_{MC}$,

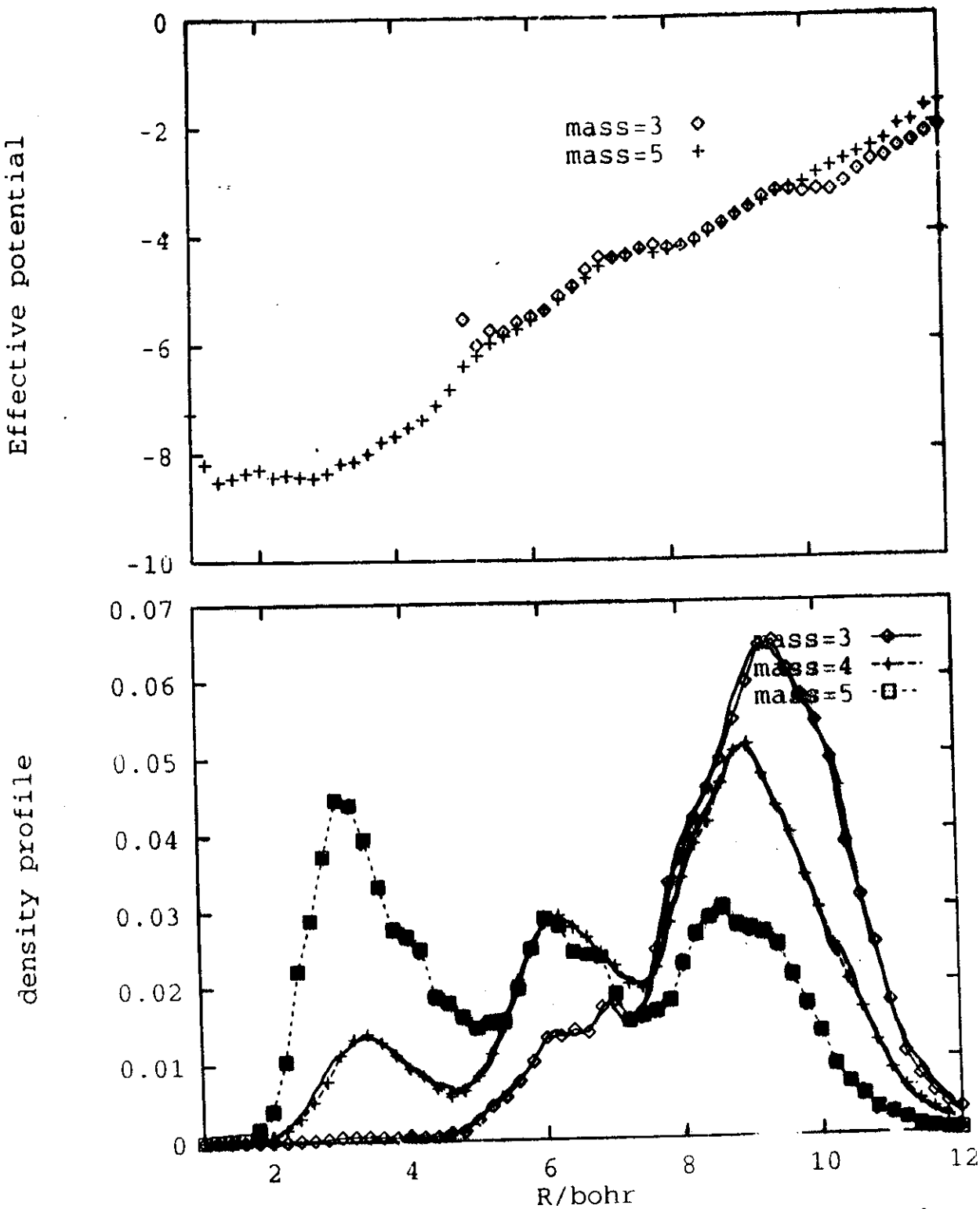

A set of effective one-particle potentials would be expected to lead to a spherically coated cluster structure

C. Chakravarty, Phys. Rev. Lett., 75, 1727 ('95)

$(o\text{-}D_2)(p\text{-}H_2)_{17}$

$T = 2.5\,K$

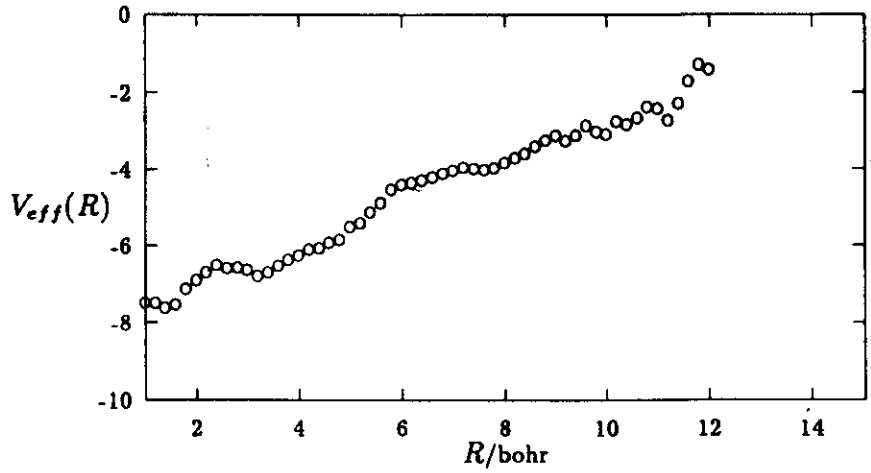

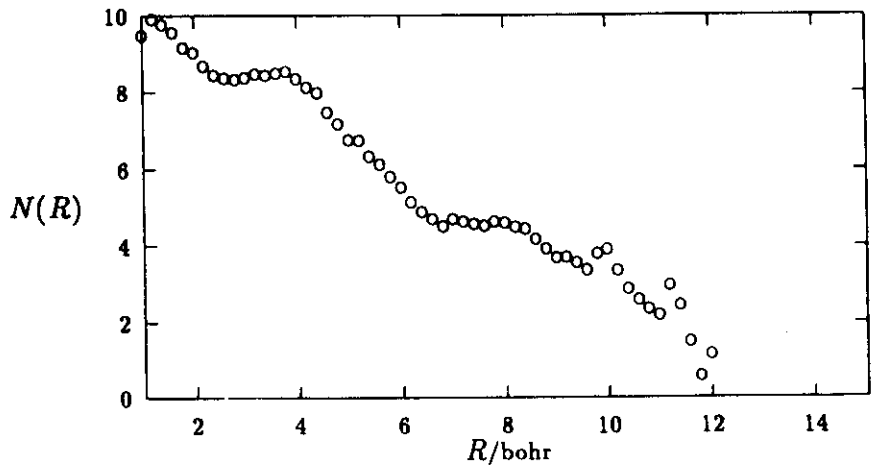

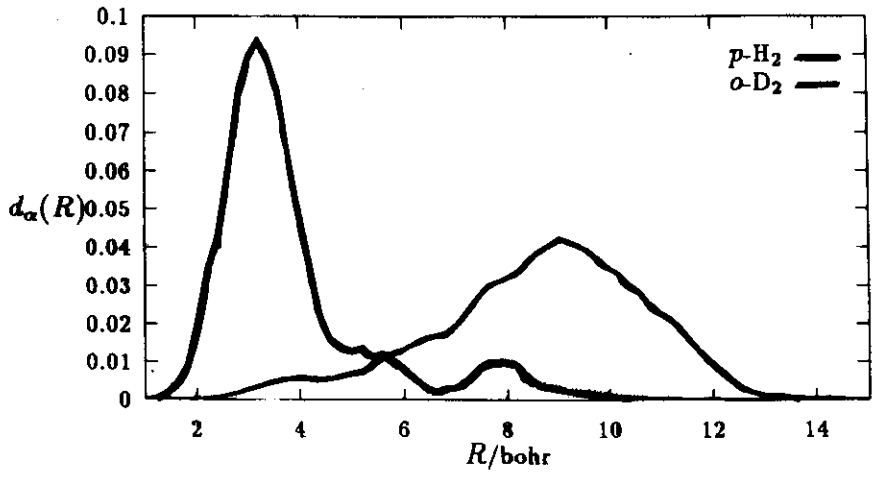

T = 2.5 K

C. Chakravarty,
Phys. Rev. Lett.,
75, 1127 ('95)

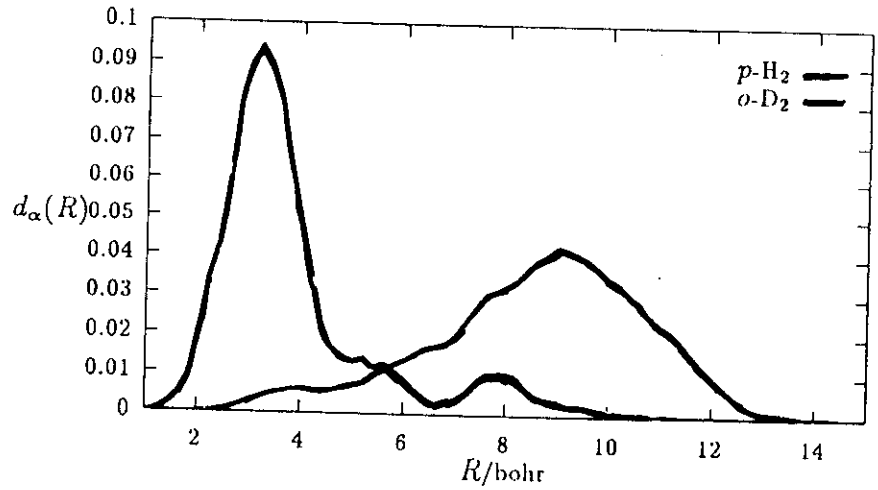

$(o\text{-}D_2)(p\text{-}H_2)_{17}$

$R_D = 0.68\sigma$
$R_H = 1.52\sigma$

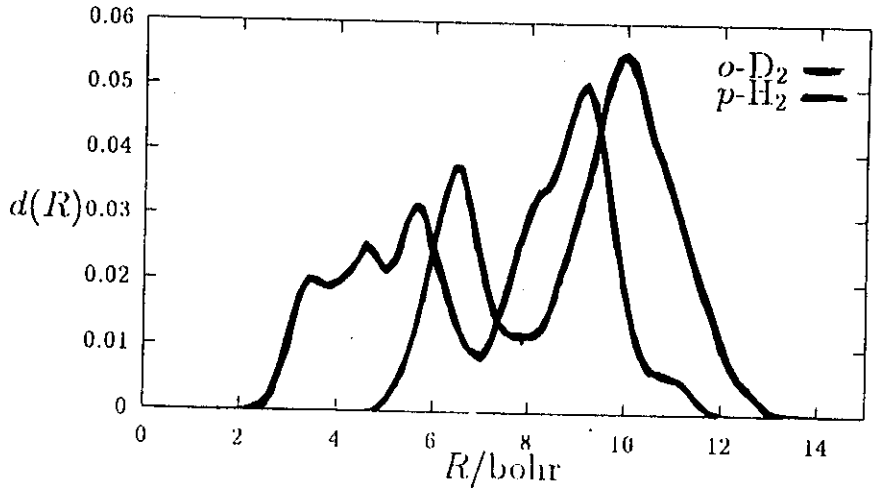

$(o\text{-}D_2)_9(p\text{-}H_2)_9$

$R_D = 1.26\sigma$
$R_H = 1.60\sigma$

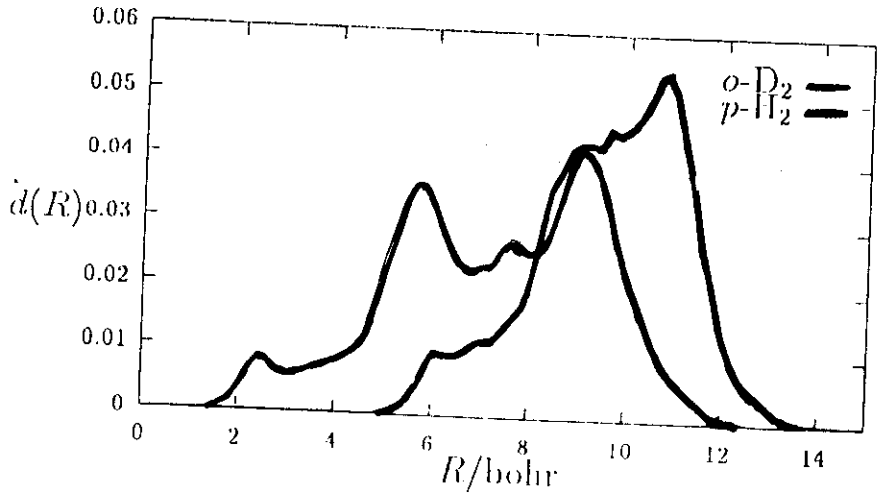

$(o\text{-}D_2)_{13}(p\text{-}H_2)_5$

$R_D = 1.28\sigma$
$R_H = 1.90\sigma$

C. Chakravarty
J. Chem. Physics, 104, 7223 ('96)

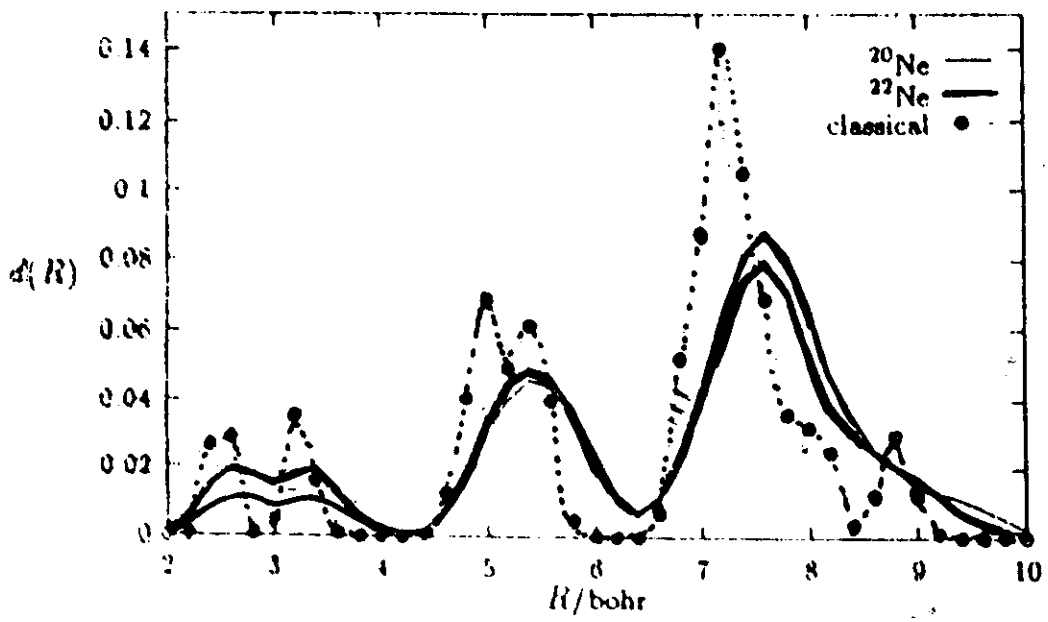
0.14
0.12
0.1
0.08
0.06
0.04
0.02
0
$d\sigma(R)$
2
3
4
5
6
7
8
9
10
R/bohr
^{20}Ne
^{22}Ne
classical

DYNAMICAL QUANTITIES

Dynamical Correlation Functions:

$$C_{AB}(t) = \langle A(0)\, B(t) \rangle$$

$$= \frac{1}{Z} \mathrm{Tr} \left\{ e^{-\beta \hat{H}} \hat{A}\, e^{+i\hat{H}t} \hat{B}\, e^{-i\hat{H}t/\hbar} \right\}$$

Real time propagator

$$\langle \vec{x} | e^{-i\hat{H}t/\hbar} | \vec{x} \rangle = \int \mathcal{D}(x(t))\, e^{i S(x(t))}$$

Leads to complex, oscillatory weight function in the Monte Carlo scheme.

Real time

$$C_{AB}(t) = \sum_{n=-\infty}^{+\infty} c(\Omega_n)\, e^{-i\Omega_n t}$$

$$C_{AB}(-it) = \sum_{n=-\infty}^{+\infty} c(\Omega_n)\, e^{-\Omega_n t}$$

Analytic Continuation

Maximum Entropy methods.

Short-time approximations.

INSTANTANEOUS NORMAL MODE SPECTRA

CLASSICAL LIQUIDS

Quadratic Expansion of Potential Energy at any instant:

$$V(\vec{R}_t) \approx V(\vec{R}_0) - \vec{F} \cdot (\vec{R}_t - \vec{R}_0) + \frac{1}{2} (\vec{R}_t - \vec{R}_0) \cdot \underline{\underline{D}} \cdot (\vec{R}_t - \vec{R}_0)$$

$\underline{\underline{D}}$: Hessian matrix

Eigenfunctions of $\underline{\underline{D}}$: Instantaneous Normal Modes & Eigenvalues

INM Spectrum is an equilibrium quantity and.

can be defined in any ensemble

R. M. Stratt
T. Keyes

Short-time dynamics

$$x_\alpha(t) = q_\alpha(t) + f_\alpha / \omega_\alpha^2$$

$$\cdot x_\alpha(t) = x_\alpha(0) \cos(\omega_\alpha t) + [v_\alpha(0)/\omega_\alpha] \sin(\omega_\alpha t)$$

$$v_\alpha(t) = v_\alpha(0) \cos(\omega_\alpha t) - \omega_\alpha x_\alpha(0) \sin(\omega_\alpha t)$$

Fraction of imaginary frequency modes, f_u

- regions of negative curvature
- unstable, barrier-crossing modes
- shoulder modes: anharmonicities in potential energy surface
- self-diffusion coefficients

Measure of the rigidity of the system

Einstein frequency: $\omega_E^2 = \int \omega^2 p(\omega) d\omega$

$$\omega_E \propto \sqrt{\frac{\langle v^2 \rangle}{m}}$$

Short-time velocity autocorrelation function

$$C_v(t) = k_B T \int_{\text{real}} \rho(\omega) \cos(\omega t) \, d\omega$$

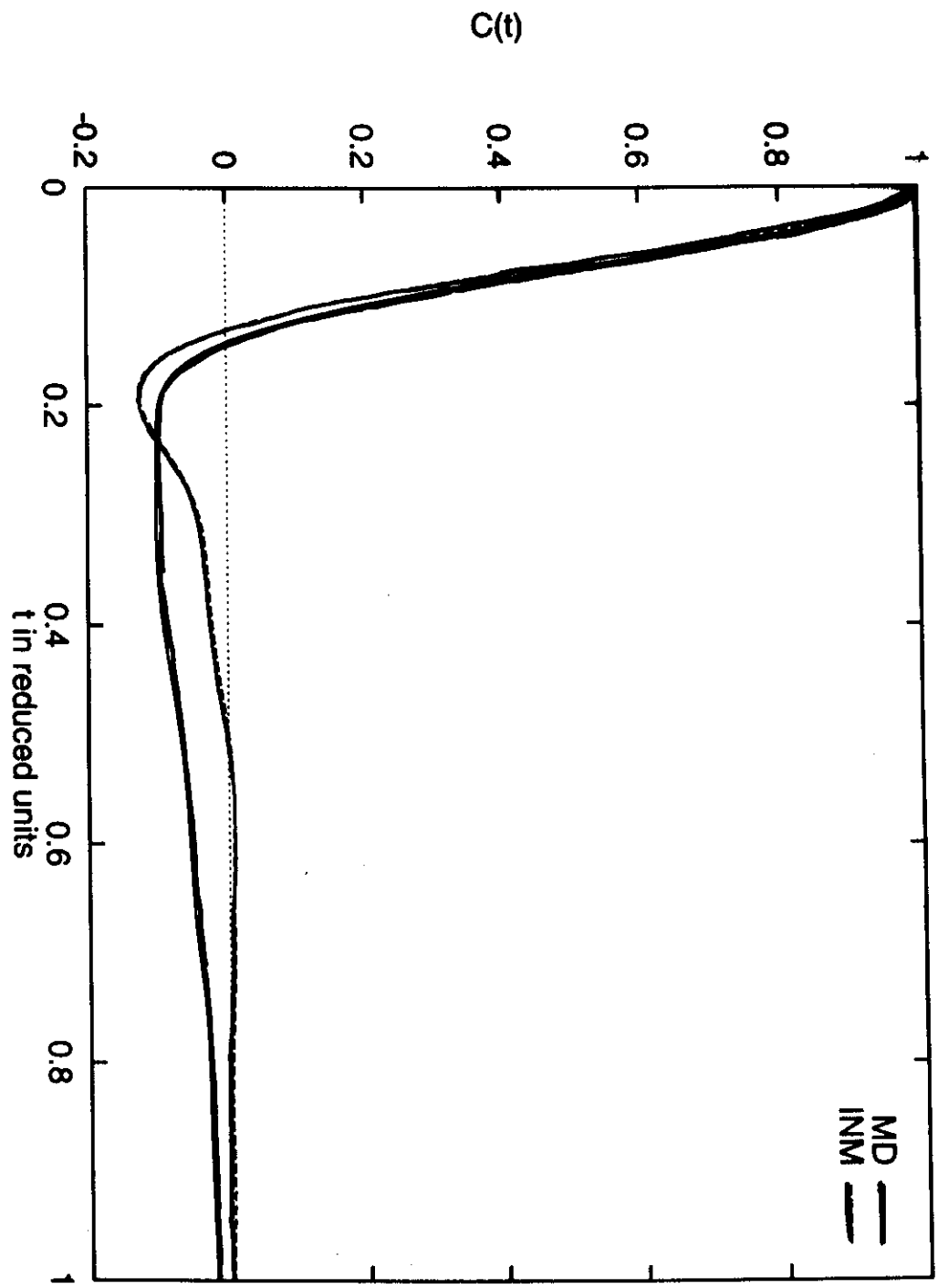
C(t)
-0.2
0
0.2
0.4
0.6
0.8
1
0
0.2
0.4
0.6
0.8
1
t in reduced units
MD
INM

NaCl melt:

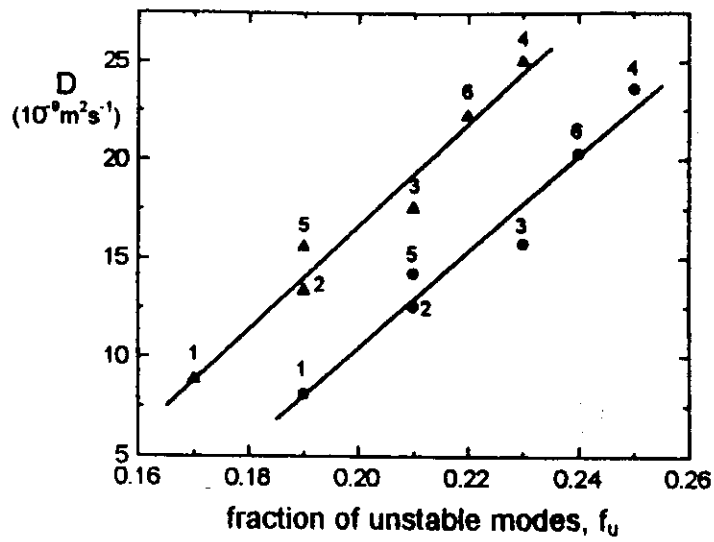

▲ cations

● anion

1 1123 K.
2 1377 K
3 1600 K
4 2056 K
5 1406 K
6 1678 K

Ribeiro & Madden, J. Chem. Phys. May '97.

INM Spectra

$kT/\varepsilon = 0.1$, $(LJ)_{13}$, $\varepsilon = 34.2\,K$, $\sigma = 2.96\,\text{Å}$

Classical

$m = 40$ amu

$\Lambda = 0.064$

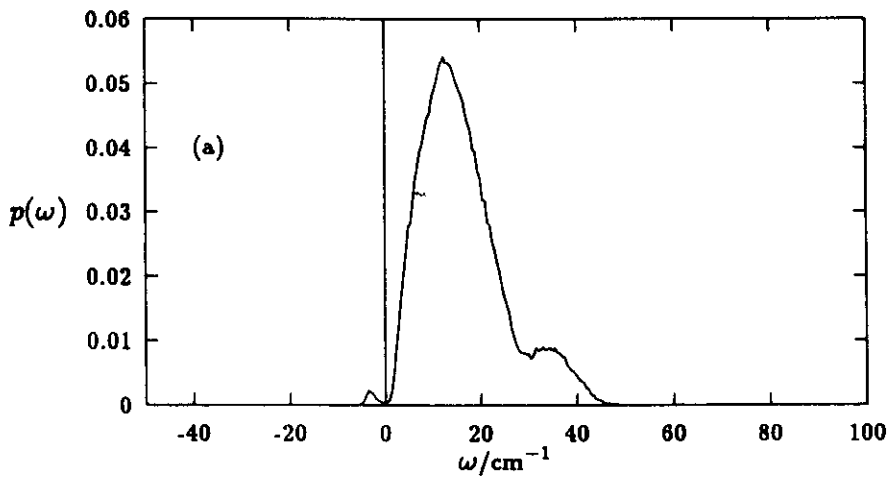

Quantum

$m = 40$ amu.

$\Lambda = 0.064$

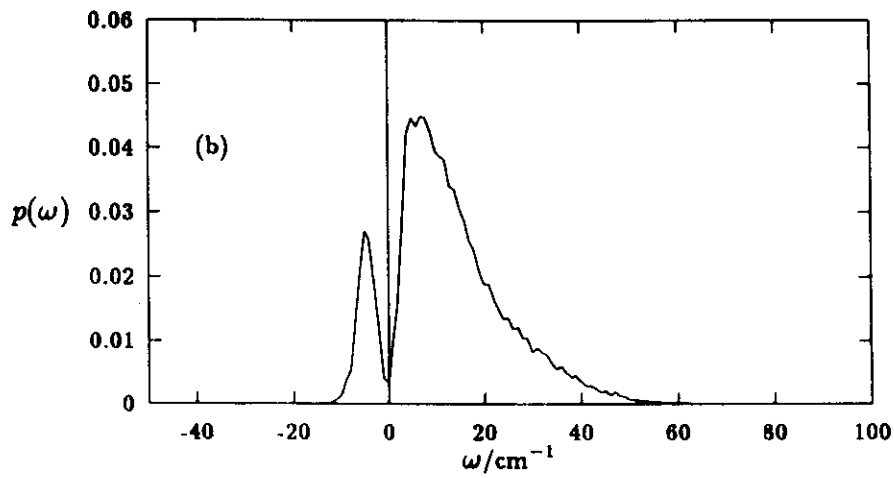

Quantum

$m = 2$ amu

$\Lambda = 0.284$

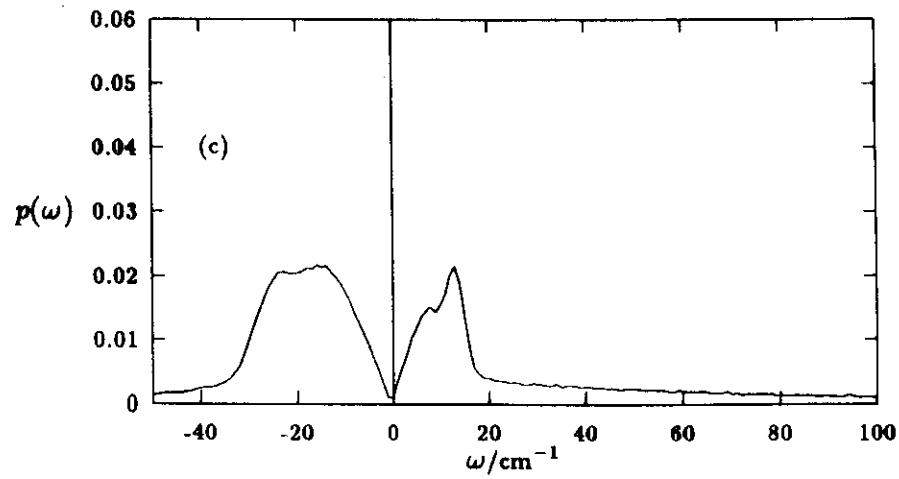

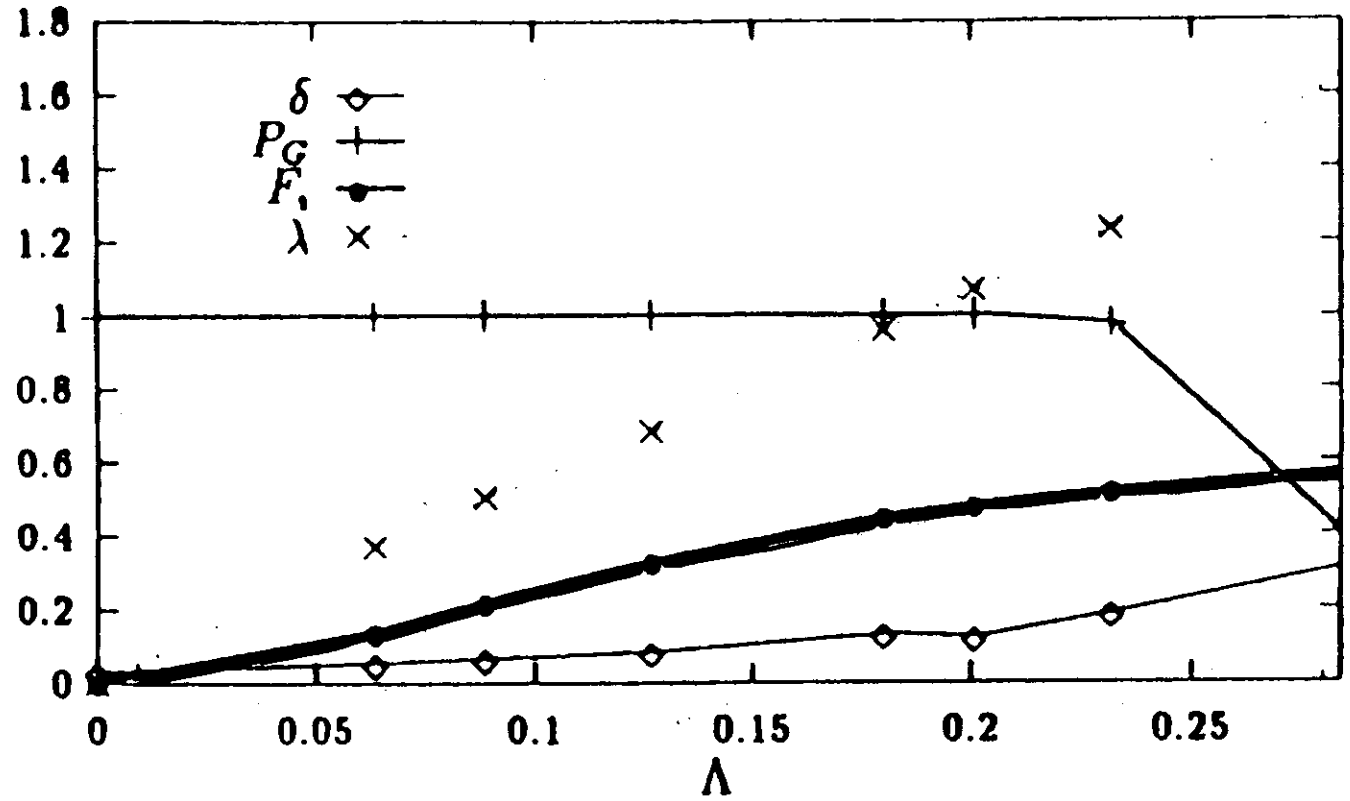

FIG. 1. Markers for the quantum cluster solid–liquid transition as a function of the de Boer parameter Λ: the probability of occupancy of the global minimum, P_G, the Lindemann index, δ, and the fraction of imaginary frequencies in the INM spectra, F_l. Also shown is the average root mean square width of quantum paths, λ, in atomic units.

HELIUM IN ZEOLITES

Experiments

- Modification of the superfluid transition in confining media (Vycor, aerogel, zeolites, fullerites)

- Adsorption isotherms, specific heats etc for ^3He and ^4He

- Neutron diffraction: He / Ne in zeolites, adsorption sites, delocaligation

SILICALITE

- pure silica zeolite.
- Pore volume ≈ 30%.
- Orthorhombic (space group : Pnma)
- Unit cell : $a = 20.07\ \text{Å}$, $b = 19.92\ \text{Å}$ and $c = 13.42\ \text{Å}$
- Straight channels parallel to the (010) - direction
  Zigzag " " " " (100) - direction.

HELIUM - SILICALITE INTERACTION

- Kiselov Models:
  - Dispersion interaction between O & rare-gas

$$V_D = 4\,\varepsilon_{OR} \sum_j \left(\frac{\sigma_{OR}^{12}}{r_{ij}^{12}} - \frac{\sigma_{OR}^{6}}{r_{ij}^{6}} \right)$$

    Can derive LJ parameters using various combining rules.
  - Partial charges + polarizable atoms on framework

    - negligible for pure silica zeolites.
  - Silicon atoms completely shielded by oxygen tetrahedra.

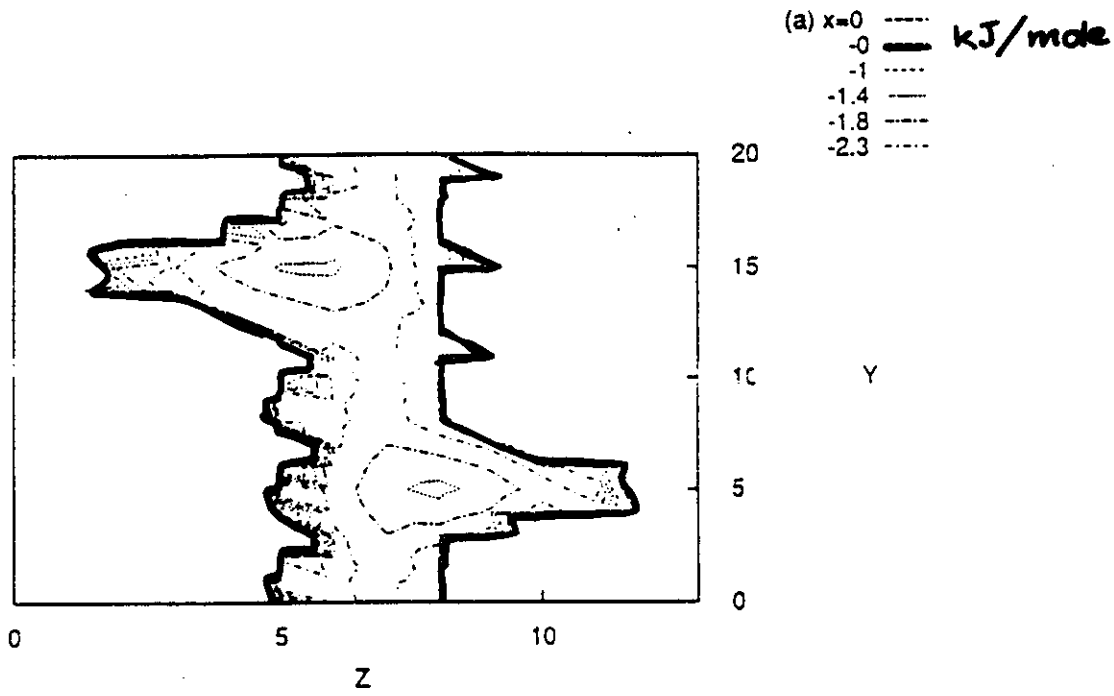

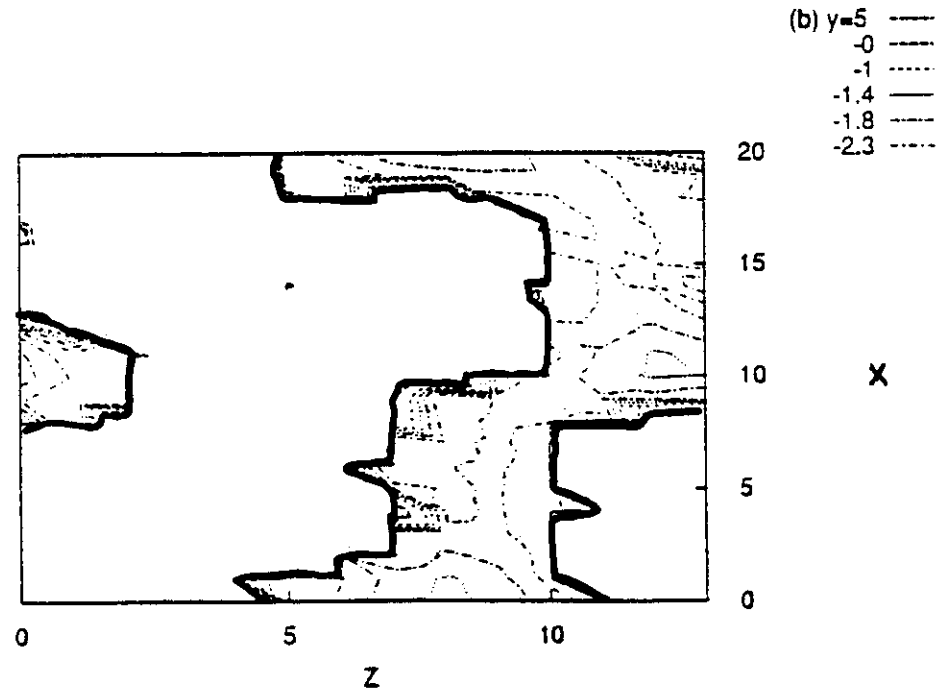

Figure 1. Contour plots of the helium–silicalite potential energy surface using potential parameters in set B: (a) $x = 0$ Å, (b) $y = 5$ Å planes. All distances are in angstroms.

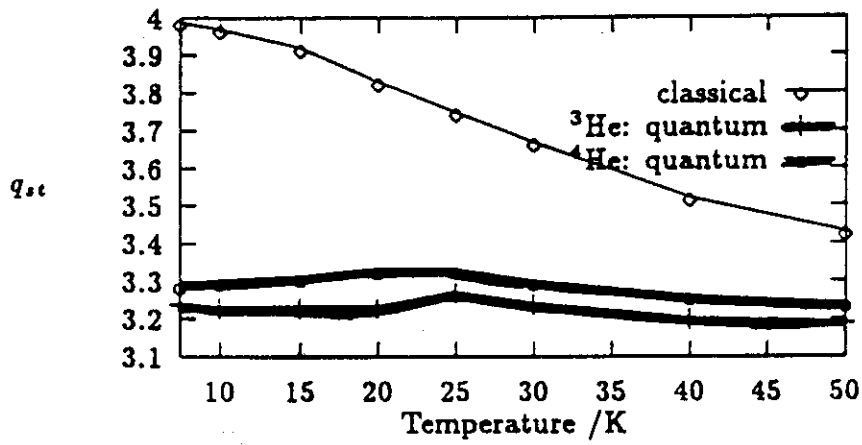

Figure 1: Isosteric heats of adsorption, q_{st}, (in kJ mol^{-1}) for helium in silicalite in the dilute limit. Error bars for q_{st} are less than 3% for all the simulations.

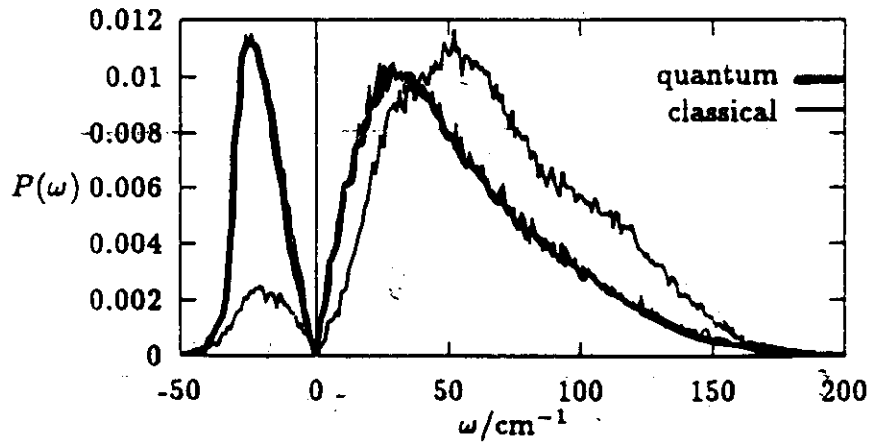

Figure 2: INM Spectra for a single helium atom in a silicalite unit cell at 10 K from quantum and classical Monte Carlo simulations. Note that imaginary frequencies are shown of the negative frequency axis for convenience.

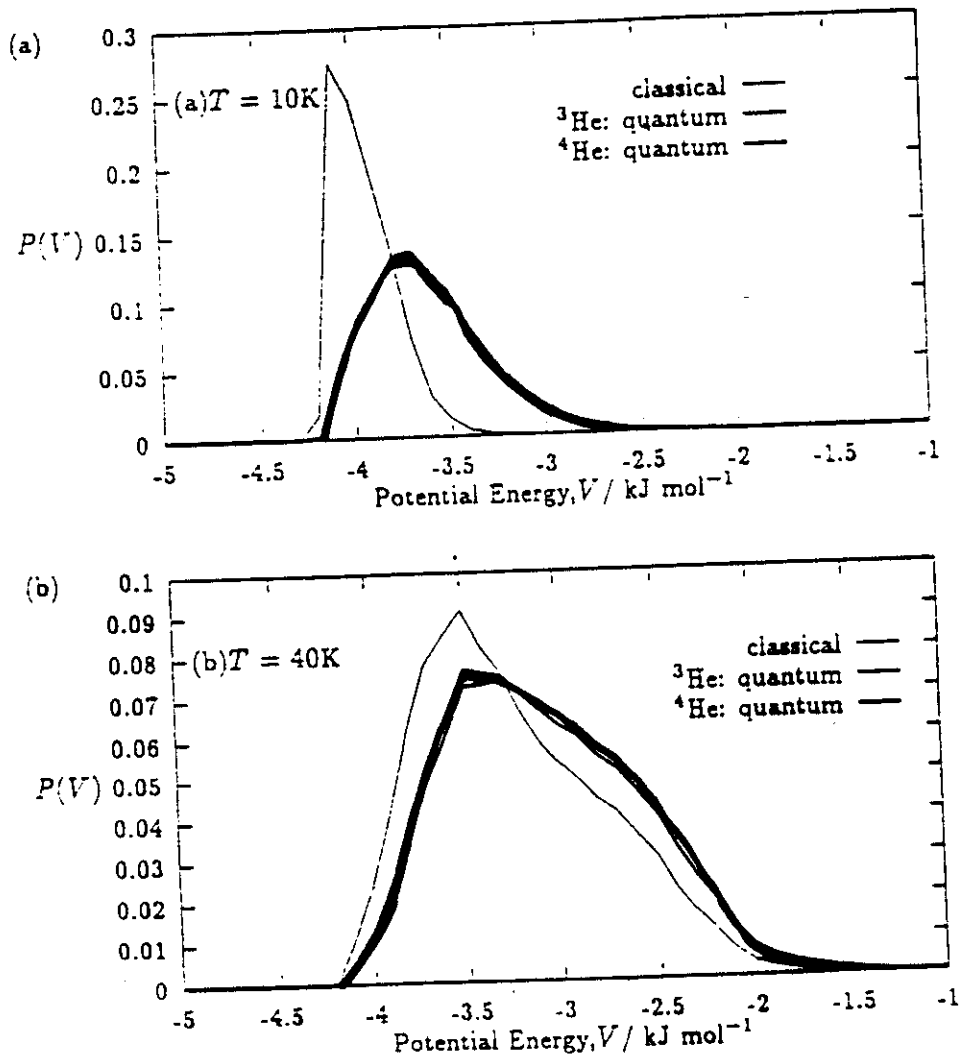

Figure 6. Potential energy distributions, $P(V)$, derived from classical and quantum simulations of helium in silicalite at (a) 10 K and (b) 40 K.